Direct-Dynamics VTST Study of the [1,7] Hydrogen Shift in 7-Methylocta-1,3(Z),5(Z)-triene. A Model System for the Hydrogen Transfer Reaction in Previtamin D_3

S. Hosein Mousavipour,† Antonio Fernández-Ramos,* Rubén Meana-Pañeda, Emilio Martínez-Núñez, Saulo A. Vázquez, and Miguel A. Ríos*

Departamento de Química Física, Facultade de Química, Universidade de Santiago de Compostela, 15782 Santiago de Compostela, Spain

Received: October 4, 2006; In Final Form: November 9, 2006

Direct-dynamics canonical variational transition-state theory calculations with microcanonically optimized multidimensional transmission coefficient (CVT/μOMT) for tunneling were carried out at the MPWB1K/6-31+G(d,p) level to study the [1,7] sigmatropic hydrogen rearrangement in 7-methylocta-1,3(Z),5(Z)-triene. This compound has seven conformers, of which only one leads to products, although all of them have to be included in the theoretical treatment. The calculated CVT/μOMT rate constants are in good agreement with the available experimental data. To try to understand the role of tunneling in the hydrogen shift reaction, we have also calculated the thermal rate constants for the monodeuterated compound in the interval $T = 333.2-388.2$ K. This allowed us to evaluate primary kinetic isotope effects (KIEs) and make a direct comparison with the experiment. Our calculations show that both the large measured KIE and the large measured difference in the activation energies between the deuterated and root compounds are due to the quantum tunneling. The tunneling contribution to the KIE becomes noticeable only when the coupling between the reaction coordinate and the transverse modes is taken into account. Our results confirm previous experimental and theoretical works, which guessed that the obtained kinetic parameters pointed to a reaction with an important contribution due to tunneling. The above conclusion would be essentially valid for the case of the [1,7] hydrogen shift in previtamin D_3 because of the similarity to the studied model system.

1. Introduction

Sigmatropic hydrogen shifts are hydrogen transfer reactions that play an important role in some biologically relevant processes. A clear example is the [1,7] hydrogen shift in previtamin D_3.[1] The vitamin is formed from 7-dehydrocholesterol in two well-defined steps.[2] The first step is a photochemical process in which cholesterol is transformed into previtamin D_3 when irradiated with ultraviolet light. In the second step, this previtamin leads to vitamin D_3 by thermal isomerization, i.e., by antarafacial [1,7] hydrogen shift between carbons C_9 and C_{19}, as indicated in Scheme 1.

The [1,7] hydrogen shift involves the transfer of a light particle between two heavy atoms; tunneling through the barrier may be of importance. In this context, the measurement of kinetic isotope effects (KIEs) is a very useful tool in the understanding of the significance of tunneling in hydrogen transfer reactions.[3] Usually, a large KIE indicates the presence of tunneling because hydrogen tunnels through a classical barrier better than deuterium, so the rate constant of the process for the former atom increases more than for the latter. This would be always the case if tunneling were a one-dimensional effect. However, because of its multidimensional nature, there are cases for which tunneling may be important even with low KIEs.[4] One of the advantages of performing theoretical reaction dynamics studies is the possibility of calculating separately the effect of different contributions to the KIE, i.e., the classical (rotational, vibrational, and electronic) and the quantum (tunneling) contributions. In particular, variational transition-state theory with multidimensional tunneling corrections (VTST/MT) has proven to be a powerful and useful tool.[5]

SCHEME 1: Thermal Isomerization of Previtamin D_3 to Vitamin D_3

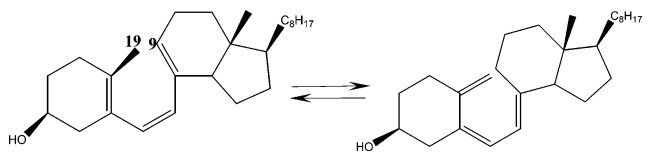

Previtamin D_3 **Vitamin D_3**

Vitamin D_3 is a big molecule to be treated with semiclassical direct-dynamics models, and even if we use density functional theory (DFT) methods for the electronic structure calculations, these would be very expensive in computer time. Of course, one can use semiempirical methods with specific reaction parameters (SRPs),[6] but in this case, we preferred to use straight high-level direct dynamics, because it is easy to find good models to describe the main features of the [1,7] hydrogen shift in the previtamin D_3. One model system with these characteristics is 1,3(Z),5(Z)-octatriene, because it contains the essence of the hydrogen transfer active site. Kinetic isotope effects on the hydrogen shift of this system were measured by Baldwin and Reddy[7] in the range of temperatures 333.2−388.2 K, although these authors could not draw firm conclusions about the thermal dependence of the KIEs because of the complexity of the kinetics and the difficulty to distinguish between primary and secondary KIEs. In this aspect, an easier system to study, although slightly larger, is the hydrogen shift in 7-methylocta-

* To whom correspondence should be addressed. E-mail for A. F.-R.: qftramos@usc.es. E-mail for M. A. R.: qftrios@usc.es.

† Permanent address: Department of Chemistry, College of Sciences, Shiraz University, Shiraz, I. R. Iran.

10.1021/jp0665269 CCC: $37.00
Published on Web 01/05/2007

1,3(Z),5(Z)-triene, because the reaction leads to a single conformer called 2-methylocta-2,4(Z),6(Z)-triene. In this case, it is possible to deuterate only the transferred hydrogen, so there are no contributions from secondary KIEs in the measurement. These measurements of the primary KIEs in 7-methylocta-1,3-(Z),5(Z)-triene were also carried out by Baldwin and Reddy[8] in the range of temperatures 333.2−388.2 K, and in this case, it was possible to easily measure the temperature dependence of the rate constants. Those authors obtained KIEs of 7.0 at $T = 333.2$ K and 4.6 at $T = 388$ K, respectively, and concluded that tunneling effects for this reaction are substantial because the difference between the activation energies for the root and deuterated compounds is large. Jensen[9] and Hess[10] independently corroborated this conclusion by carrying out electronic structure calculations. The former applied the conventional transition-state theory to the reaction after performing B3LYP/6-31+G* calculations on the stationary points. Hess calculated a KIE of 3.89 at 333.2 K, which is about half the experimental value obtained by Baldwin and Reddy,[8] concluding that the difference is due to the neglect of tunneling in his calculation.

The above KIEs are very similar to those measured by Okamura et al.[11] for the [1,7]-sigmatropic hydrogen shift of previtamin D_3 to vitamin D_3, which range from 7.4 at $T = 333.2$ K to 6.1 at $T = 358.7$ K. They used a pentadeuterio derivative of previtamin D_3, but in this case, a negligible secondary KIE is expected. The similarity between the KIEs indicates that tunneling may also play an important role in this case and that 7-methylocta-1,3(Z),5(Z)-triene is a good system to model the hydrogen shift process in previtamin D_3. Therefore, the aim of this paper is to use VTST/MT to get insight into the role played by tunneling in the [1,7] hydrogen shift of 7-methylocta-1,3(Z),5(Z)-triene by analyzing the calculated KIEs. Because of the similarities between this molecule and previtamin D_3, the conclusions obtained would be common to both systems.

2. Computational Details

All the electronic structure calculations have been performed at the MPWB1K level[12] with the 6-31+G(d,p) basis set,[13] also called DIDZ. MPWB1K is a DFT method based on the Perdew and Wang 1991 exchange functional[14] (MPW) and Becke's 1995 meta correlation functional (B95),[15] which has been optimized for kinetics calculations, so we also expect a good performance of the method in this case. The geometry optimizations and frequency calculations at the stationary points were performed with Gaussian03.[16]

All dynamics calculations were carried out by VTST/MT using the MPWB1K/DIDZ level to build the potential energy surface. VTST/MT improves conventional transition-state theory in two aspects:[17,18] (a) it minimizes the recrossing by variationally locating the transition-state dividing surface at an optimized position orthogonal to the minimum energy path (MEP); and (b) it incorporates multidimensional tunneling effects into the reaction coordinate by a multiplicative transmission coefficient. The MEP was followed in redundant curvilinear (internal) coordinates[19] by using the Page−McIver algorithm.[20] The advantage of using internal coordinates along the MEP is that it provides more reliable normal-mode frequencies along the MEP than rectilinear (Cartesian) coordinates.[21,22] A converged MEP was obtained with a step size of $0.01a_o$, scale mass $\mu = 1$ amu, and Hessian calculations every nine steps. All frequencies were scaled by the recommended factor of 0.9537.[12]

Variational effects were incorporated by the canonical variational transition-state theory (CVT),[23−25] in which the flux is minimized for a canonical ensemble. The CVT rate constant, $k^{CVT}(T)$, at temperature T, can be obtained as the minimum of the generalized transition-state theory rate constant, $k^{GT}(T, s)$, as a function of s, that is,

$$k^{CVT}(T) = \min_s k^{GT}(T,s) = \sigma \frac{1}{\beta h} \frac{Q^{GT}(T,s_*^{CVT})}{Q^R(T)} \exp[-\beta V_{MEP}(s_*^{CVT})] \quad (1)$$

where s is the arc length along the MEP measured from the saddle point; s_*^{CVT} is the value of s at which $k^{GT}(T, s)$ has a minimum; σ is the symmetry number; $\beta = (k_B T)^{-1}$, where k_B is the Boltzmann's constant; $V_{MEP}(s_*^{CVT})$ is the classical MEP potential at $s = s_*^{CVT}$; and $Q^{GT}(T, s_*^{CVT})$ and $Q^R(T)$ are the internal (rotational, vibrational, and electronic) partition functions of the generalized transition state at $s = s_*^{CVT}$ and reactants, respectively.

Tunneling effects were incorporated into the thermal CVT rate constants by a multiplicative ground-state (G) transmission coefficient, $\kappa^{CVT/G}(T)$, so the final rate constant is given by

$$k^{CVT/G}(T) = \kappa^{CVT/G}(T) k^{CVT}(T) \quad (2)$$

where

$$\kappa^{CVT/G}(T) = \beta \exp\{\beta V_a^G(s^{*CVT})\} \int_{E_0}^{\infty} P^G(E)\, e^{-\beta E}\, dE \quad (3)$$

where V_a^G is the vibrationally adiabatic potential, which is given by

$$V_a^G(s) = V_{MEP}(s) + \epsilon_{int}^G(s) \quad (4)$$

where $\epsilon_{int}^G(s)$ is the internal energy (rotational and vibrational) at s, which in the ground-state approximation equals the zero-point energy (ZPE) at s. The semiclassical ground-state probability $P^G(E)$ was calculated over the vibrational adiabatic potential by optimizing microcanonically (at every energy) the largest probability between the small curvature tunneling (SCT) probability,[26] $P^{SCT}(E)$, and the large curvature tunneling (LCT) probability,[17,18,27−29] $P^{LCT}(E)$, evaluated with the LCG4 version.[29] The resulting probability is, therefore, given by

$$P^{\mu OMT}(E) = \max_E \begin{Bmatrix} P^{SCT}(E) \\ P^{LCT}(E) \end{Bmatrix} \quad (5)$$

where μOMT stands for microcanonically optimized multidimensional tunneling.[30] The semiclasical probability in the whole range of energies is given by

$$P^G(E) = \begin{Bmatrix} 0, & E < E_0 \\ \{1 + \exp[2\theta(E)]\}^{-1}, & E_0 \le E \le V^{AG} \\ 1 - P^G(2V^{AG} - E), & V^{AG} \le E \le 2V^{AG} - E_0 \\ 1, & 2V^{AG} - E_0 < E \end{Bmatrix} \quad (6)$$

where E_0 is the lowest energy at which it is possible to have tunneling, V^{AG} is the top of the vibrationally adiabatic potential, and $\theta(E)$ is the imaginary action integral. This integral in the SCT approximation is given by

$$\theta(E) = \frac{1}{\hbar} \int_{s_0}^{s_1} ds\, \{2\mu_{eff}^{SC}(s)[V_a^G(s) - E]\}^{1/2} \quad (7)$$

where s_0 and s_1 are the classical turning points and $\mu_{\mathrm{eff}}^{\mathrm{SC}}(s)$ is the effective mass, which is a function of the couplings between the reaction coordinate and the transverse modes at a given value of s. If this coupling is neglected, $\mu_{\mathrm{eff}}^{\mathrm{SC}}(s)$ equals the scaling mass and the approximation is called zero-curvature tunneling (ZCT). The probabilities evaluated under the ZCT approximation always underestimate the tunneling contribution, because the coupling curves the tunneling trajectory toward the inside of the MEP (centrifugal effect), shortening the tunneling distance.[31] In fact, the SCT trajectory is not calculated explicitly, but it has been shown that its effect can be incorporated in the effective mass, which decreases its value (decreasing the value of the imaginary integral and, therefore, increasing the tunneling probability) in regards to the constant scaling mass.

On the other hand, the evaluation of the μOMT transmission coefficients also requires the calculation of the LCT probabilities. In this case, we need more information of the potential energy surface and not just the MEP; in fact, the evaluation of $P^{\mathrm{LCT}}(E)$ can be quite expensive from the computational point of view. Recently one of us, together with Truhlar, developed an algorithm, called ILCT2D (interpolated large-curvature tunneling with a two-dimensional spline under tension), that allows the calculation of such probabilities with similar results to the full LCT calculation but about 30× faster.[32] We have used the ILCT2D algorithm in this case.

It should be noticed that the μOMT transmission coefficient is an approximation to the least-action path, which is the one that minimizes the action integral at each tunneling energy.[33] The least-action path is the best compromise between long but energetically favorable tunneling paths (like the MEP) and short but energetically unfavorable tunneling (like the linear paths). Because the explicit evaluation of the least-action path, and therefore of the least-action probability, is very difficult in systems with many degrees of freedom, the μOMT probability represents a good compromise between longer paths closer to the MEP, which are well-described by the SCT approximation, and shorter paths, which are well-described by the LCT approximation. Actually, the μOMT tranmission coefficient was as accurate as the least-action path transmission coefficient for triatomic systems when compared with quantum dynamics calculations.[34]

With these prescriptions, the calculated rate constant obtained using the transmission coefficient from the μOMT probability, $\kappa^{\mathrm{CVT}/\mu\mathrm{OMT}}(T)$, is given by

$$k^{\mathrm{CVT}/\mu\mathrm{OMT}}(T) = \kappa^{\mathrm{CVT}/\mu\mathrm{OMT}}(T) k^{\mathrm{CVT}}(T) \tag{8}$$

On the other hand, the primary total KIEs, $\eta^{\mathrm{H/D}}$, were factorized by their classical, η_{cl}, and tunneling, η_{tun}, contributions, that is,

$$\eta^{\mathrm{H/D}} = \frac{k_{\mathrm{H}}^{\mathrm{CVT}/\mu\mathrm{OMT}}}{k_{\mathrm{D}}^{\mathrm{CVT}/\mu\mathrm{OMT}}} = \eta_{\mathrm{tun}}\eta_{\mathrm{cl}} \tag{9}$$

where

$$\eta_{\mathrm{tun}} = \frac{\kappa_{\mathrm{H}}^{\mathrm{CVT}/\mu\mathrm{OMT}}}{\kappa_{\mathrm{D}}^{\mathrm{CVT}/\mu\mathrm{OMT}}} \tag{10}$$

and η_{cl} is given by

$$\eta_{\mathrm{cl}} = \eta_{\mathrm{var}}\eta_{\mathrm{int}} \tag{11}$$

where η_{var} and η_{int} are the variational and internal (rotational and vibrational) KIEs, respectively. The variational KIE is given by the ratio

$$\eta_{\mathrm{var}} = \frac{k_{\mathrm{H}}^{\mathrm{CVT}} k_{\mathrm{D}}^{\mathrm{TST}}}{k_{\mathrm{D}}^{\mathrm{CVT}} k_{\mathrm{H}}^{\mathrm{TST}}} \tag{12}$$

where k^{TST} indicates conventional TST rate constant (i.e., with the dividing surface located at the TS), whereas the KIE due to internal motions is given by

$$\eta_{\mathrm{int}} = \frac{\eta_{\mathrm{int,H}}}{\eta_{\mathrm{int,D}}} = \frac{Q_{\mathrm{rot,H}}^{\mathrm{TS}} Q_{\mathrm{rot,D}}^{\mathrm{R}}}{Q_{\mathrm{rot,D}}^{\mathrm{TS}} Q_{\mathrm{rot,H}}^{\mathrm{R}}} \frac{Q_{\mathrm{vib,H}}^{\mathrm{TS}} Q_{\mathrm{vib,D}}^{\mathrm{R}}}{Q_{\mathrm{vib,D}}^{\mathrm{TS}} Q_{\mathrm{vib,H}}^{\mathrm{R}}} \tag{13}$$

where Q_{rot} and Q_{vib} are the rotational and vibrational partition functions, respectively. The subscripts R and TS stand for reactants and transition state, respectively.

All the rate constant calculations were performed with the program GAUSSRATE9.1,[35] which is an interface between POLYRATE9.3[36] and Gaussian03.[16]

3. Results and Discussion

Figure 1 shows seven possible conformers of the 7-methylocta-1,3(Z),5(Z)-triene. According to our MPWB1K/DIDZ calculations, conformer **R1** has the most stable structure with an *s-trans*, *s-trans* configuration, in agreement with the B3LYP/6-31G* calculations of Hess.[10] Conformer **R1** can lead to the *s-trans*, *s-cis* structure (conformer **R2**) or to the *s-cis*, *s-trans* structure (conformer **R3**). Both conformers (**2** and **3**) can lead to the reacting *s-cis*, *s-cis* configuration (conformer **R7**) via rotation around one of the single bonds. Also, there is a possibility for conformer **R1** to transform into conformer **R4** by rotation around the C_6-C_7 single bond and for **R4** to transform into conformers **R2** and **R3** via the intermediate conformations **R6** and **R5**, respectively. Some of the key distances and angles of the seven conformers, together with all the transition states involved in the interconversion between conformers, are listed in Table 1.

Conformer **R7** has the most suitable configuration for the [1,7] hydrogen shift with a C_1-H_{17} distance of 3.253 Å, although the transfer is also possible from conformer **R2**. The direct product of conformer **R7** through **TS7** is 2-methylocta-2,4(Z),6(Z)-triene, which is shown as **P1** in Figure 2, whereas the direct product of conformer **R2** through **TS2** is 2-methylocta-2,4(Z),6(E)-triene, which is shown as **P2** in Figure 2. As shown in Table 1, the energetically most probable route for the hydrogen transfer is through conformer **R7**. This conformer has to surmount a classical barrier of 18.98 kcal·mol^{-1} to lead to products. In the case of conformer **R2**, the classical barrier is 42.59 kcal·mol^{-1}, and although **R2** is ∼5 kcal·mol^{-1} more stable than **R7**, the difference in the barrier heights indicates that the hydrogen shift would take place only through transition state **TS7**.

Despite the fact that there is only one relevant channel for reaction, all conformers are relevant to the dynamics because the barriers of internal rotation around the single bonds among the different conformers are much smaller than the barrier for reaction. As a consequence, all the conformers can be easily reached and all the regions in phase space related to reactants

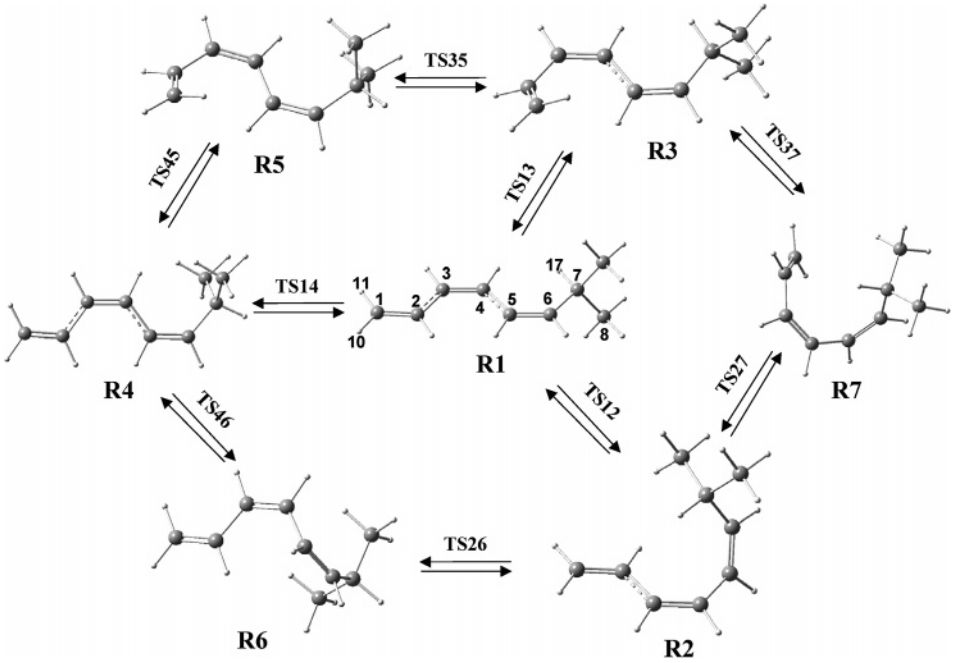

Figure 1. Seven conformers of 7-methylocta-1,3(Z),5(Z)-triene. The arrows between two structures indicate that there is a transition state connecting them. Details about the geometries and relative energies of the conformers and the transition states are given in Table 1.

TABLE 1: Relative Classical Potential Energies (in kcal/mol) and Main Geometric Parameters (Distances in Å and Angles in Degrees) of the Stationary Points Involved in the [1,7] Hydrogen Shift in 7-Methylocta-1,3(Z),5(Z)-triene Calculated at the MPWB1K/6-31+G(d,p) Level; Numbering as for Structure R1 in Figure 1

structure	energy	ϕ_1[a]	ϕ_2[a]	ϕ_3[a]	α_1[a]	α_2[a]	α_3[a]	d(C_7-H_{17})	d(C_1-C_7)	d(C_1-H_{17})
R1	0.00	179.8	179.9	−2.5	109.8	117.1	110.6	1.088	6.749	6.411
R2	2.78	−175.9	55.7	−8.0	109.1	117.1	110.2	1.088	4.311	3.529
R3	3.18	40.0	−171.4	0.1	109.6	117.3	110.5	1.089	5.614	5.532
R4	3.31	180.0	180.0	180.0	105.9	117.1	111.7	1.090	6.791	7.725
R5	6.40	39.54	−169.2	173.3	106.0	117.3	111.6	1.090	5.596	6.352
R6	7.44	179.34	97.7	164.2	106.3	117.1	110.8	1.091	5.430	6.424
R7	7.70	36.81	58.6	−8.7	108.7	117.5	110.5	1.088	3.677	3.253
TS12	4.81	179.7	98.8	4.0	108.3	117.0	110.8	1.085	5.371	4.937
TS13	6.07	98.1	178.7	0.3	109.7	117.3	110.5	1.089	6.191	6.019
TS14	4.55	−179.6	−177.7	−89.1	107.2	117.1	109.5	1.094	6.857	7.210
TS26	7.76	−179.1	96.8	−122.2	105.9	117.1	110.6	1.090	5.509	5.539
TS27	10.37	104.3	59.5	−3.7	108.7	117.2	110.3	1.089	4.493	4.022
TS35	7.81	38.8	−167.1	81.6	107.2	117.3	109.5	1.094	5.614	5.652
TS37	8.80	18.7	93.5	6.2	108.2	117.1	110.8	1.090	4.350	4.261
TS45	9.36	98.2	179.0	−179.7	106.0	117.3	111.6	1.090	6.219	7.064
TS46	7.47	179.2	105.4	164.9	106.5	117.1	110.8	1.091	5.605	6.602
TS7	26.68	10.3	22.0	−64.5	100.0	114.8	114.0	1.330	2.641	1.368
P1	0.58	0.04	4.3	−96.8	76.5	109.1	115.1	3.028	3.518	1.091
TS2	45.37	−127.1	27.7	−80.9	103.0	114.8	114.3	1.434	2.756	1.382
P2	0.67	176.8	4.8	−65.1	101.0	108.2	115.5	4.524	4.598	1.090

[a] $\phi_1 = \phi(C_1-C_2-C_3-C_4)$, $\phi_2 = \phi(C_3-C_4-C_5-C_6)$, $\phi_3 = \phi(C_5-C_6-C_7-H_{17})$, $\alpha_1 = \alpha(C_6-C_7-H_{17})$, $\alpha_1 = \alpha(H_{10}-C_1-H_{11})$, and $\alpha_1 = \alpha(C_8-C_7-C_9)$.

should be included.[37] The CVT thermal rate constant in a case like this is given by[38]

$$k^{\mathrm{CVT}}(T) = \frac{1}{\beta h} \frac{Q^{\mathrm{GT}}(T,s_*^{\mathrm{CVT}})}{\sum_{i=1}^{7} (1/\sigma^{\mathbf{R}_i}) Q^{\mathbf{R}_i}(T)\, \mathrm{e}^{-\beta \Delta E_{\mathrm{Ri}}}} \exp[-\beta V_{\mathrm{MEP}}(s_*^{\mathrm{CVT}})] \tag{14}$$

where the sum runs over the seven conformers ($i = 1, ..., 7$), with $Q^{\mathbf{R}_i}(T)$ and $\Delta E_{\mathbf{R}_i}$ being the partition function of conformer $\mathbf{R}_i$ and the relative energy of conformer $\mathbf{R}_i$ regarding the most stable conformer, respectively. By contrast to eq 1, in eq 14 there is a symmetry number for each of the conformers, $\sigma^{\mathbf{R}_i}$, which is defined as the quotient between the symmetry number due to rotation of reactant $\mathbf{R}_i$ and that of the generalized transition state at $s = s_*^{\mathrm{CVT}}$. In this case, all symmetry numbers are unity. The value of the MEP at $s = s_*^{\mathrm{CVT}}$ is also referred to the most stable conformer, which in this case is **R1**. On the other hand, the aspects related to tunneling are unaltered by the number of conformers because the [1,7] hydrogen shift involves the participation of only one of the conformers. Therefore, we still make use of eq 8, but using eq 14 instead of eq 1 for the evaluation of the CVT thermal rate constants.

The calculated thermal rate constants are listed in Table 2 and plotted in Figure 3. The CVT/μOMT values are roughly about 2× lower than the experimental ones for both the hydrogen and deuterium transfers. Variational effects are not very important; this is usually the case for hydrogen transfer reactions with relatively large barriers, because these reactions present tight transition states. As shown in Table 3, the

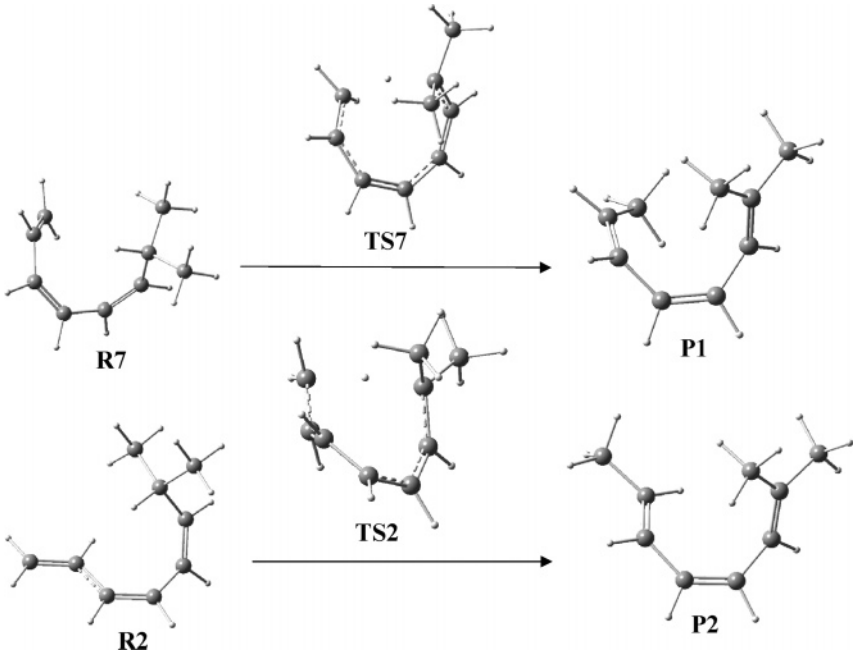

Figure 2. Structures of the two reactive conformers leading to products by [1,7] hydrogen shift. Details about the geometries and relative energies are given in Table 1.

TABLE 2: Calculated (Columns 2, 3, and 4) and Experimental (Column 5) Thermal Rate Constants (in s^{-1}) for the [1,7] Hydrogen (and Deuterium) Shift in 7-Methylocta-1,3(Z),5(Z)-triene

T (K)	TST	CVT	CVT/μOMT	exp[a]
		k_H		
298.2	6.52×10^{-8}	6.38×10^{-8}	4.79×10^{-7}	
333.2	4.69×10^{-6}	4.59×10^{-6}	2.20×10^{-5}	5.6×10^{-5}
348.2	2.22×10^{-5}	2.18×10^{-5}	9.07×10^{-5}	2.14×10^{-4}
368.2	1.46×10^{-4}	1.43×10^{-4}	5.05×10^{-4}	1.16×10^{-3}
388.2	7.84×10^{-4}	7.70×10^{-4}	2.37×10^{-3}	5.51×10^{-3}
400.0	1.95×10^{-3}	1.92×10^{-3}	5.51×10^{-3}	
		k_D		
298.2	1.47×10^{-8}	1.46×10^{-8}	7.08×10^{-8}	
333.2	1.23×10^{-6}	1.23×10^{-6}	4.12×10^{-6}	8.0×10^{-6}
348.2	6.20×10^{-6}	6.17×10^{-6}	1.84×10^{-5}	3.3×10^{-5}
368.2	4.35×10^{-5}	4.33×10^{-5}	1.13×10^{-4}	2.21×10^{-4}
388.2	2.49×10^{-4}	2.48×10^{-4}	5.80×10^{-4}	1.21×10^{-3}
400.0	6.43×10^{-4}	6.40×10^{-4}	1.42×10^{-3}	

[a] From ref 8.

calculated activation energies for the hydrogen shift are a little bit larger than the experimental ones, whereas those for the deuterium shift are slightly lower. These differences in the activation energies would affect the KIEs, although the overall agreement between theory and experiment is good, considering the size of the model system. Hess[10] calculated at the B3LYP/6-31+G* level a difference in activation energies $E_a^D - E_a^H = 0.9$ kcal·mol^{-1}. This value coincides with our calculated "classical" CVT value. When tunneling through the reaction coordinate barrier is taken into account, the difference $E_a^D - E_a^H$ increases. When the contribution of the ZCT transmission coefficients is included, the effect is almost negligible (0.04 kcal·mol^{-1}), but when we use the μOMT transmission coefficients, the difference increases to 0.41 kcal·mol^{-1}. In any case, the difference $E_a^D - E_a^H$ (1.29 kcal·mol^{-1}) is still small when compared with 2.0 kcal·mol^{-1} obtained by Baldwin and Reddy,[8] but still within the 95% confidence interval proposed by those authors, which is ± 0.9 kcal·mol^{-1}. From the above numbers, although the ZCT transmission coefficients are larger than 2 at 333.2 K (see Table 4), there is no increase in the difference $E_a^D - E_a^H$, and only when the coupling between the reaction coordinate and the transverse modes is included, the difference is noticeable with respect to the classical value. Another effect of the coupling is that the μOMT transmission coefficients are larger than the ZCT transmission coefficients, although the former are essentially well-reproduced by the SCT values, as shown in Table 4.

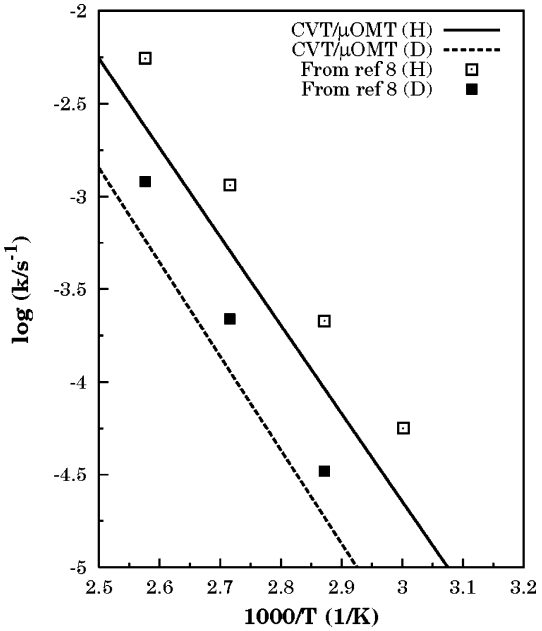

Figure 3. Thermal rate constants calculated in this work by the CVT/μOMT method for the hydrogen (solid line) and deuterium (dashed line) shift reactions of 7-methylocta-1,3(Z),5(Z)-triene. The experimental values (squares) are also plotted for comparison.

As we mentioned in the previous section, the SCT transmission coefficients work better than the LCT ones when the coupling is weak or intermediate, although in this case, the main reason for the similarity between the SCT and the μOMT transmission coefficients is that, for the range of temperatures studied, the energies that contribute mostly to tunneling are very close to the top of the vibrationally adiabatic potential. Actually,

TABLE 3: Arrhenius Parameters (Activation Energy, E_a, in kcal·mol^{-1}, and Logarithm of the Preexponential Factor, log(A/s^{-1}), for [1,7] Sigmatropic Hydrogen (and Deuterium) Shift Reactions[a]

	[1,7] H shift		[1,7] D shift	
	E_a	log A	E_a	log A
CVT	23.94	10.36	24.82	10.36
CVT/ZCT	22.83	10.02	23.75	10.02
CVT/μOMT	21.85	9.68	23.14	9.79
Baldwin and Reddy[8]	21.5	9.8	23.5	10.3

[a] The fit to the calculated values included only temperatures in the interval 333.2−388.2 K to get a more reliable comparison with the experimental data.

TABLE 4: Transmission Coefficients, κ, Evaluated by Different Approximations for [1,7] Hydrogen (and Deuterium) Shift in the 7-Methylocta-1,3(Z),5(Z)-triene

	κ_H				κ_D			
T (K)	ZCT	SCT	LCT	μOMT	ZCT	SCT	LCT	μOMT
298.2	3.06	7.40	3.89	7.50	2.80	4.85	3.10	4.85
333.2	2.42	4.78	2.78	4.80	2.24	3.35	2.30	3.35
348.2	2.24	4.14	2.50	4.16	2.08	2.98	2.20	2.98
368.2	2.05	3.52	2.24	3.53	1.91	2.61	2.00	2.61
388.2	1.91	3.08	2.04	3.08	1.79	2.34	1.85	2.34
400.0	1.83	2.87	1.95	2.87	1.72	2.22	1.78	2.22

at a given temperature, there is an energy at which the integral of eq 3 has a maximum. This energy is called the representative tunneling energy[39] (RTE) and at $T = 333.2$ K is 140.54 kcal·mol^{-1} and 140.00 kcal·mol^{-1} for the hydrogen and deuterium shifts, respectively. Taking into account that the maximum of the vibrational adiabatic potential is 141.94 and 140.70 kcal·mol^{-1} for the root and deuterated species, respectively, the RTE is roughly only 1.40 and 0.70 kcal·mol^{-1} below the top of the barrier for hydrogen and deuterium transfer, respectively, as shown in Figure 4. At these energies, because of the proximity of the top of the barrier, the curvature of the reaction path due to the coupling has to be small. However its influence is still important, and the SCT transmission coefficients are substantially larger than the ZCT ones. In this context, this study on the [1,7] hydrogen shift emphasizes the importance of treating tunneling phenomena as multidimensional events.

We can obtain a similar conclusion from the analysis of the KIEs, which are listed in Table 5. At $T = 333.2$, the classical KIE is only 3.73, which is quite close to the value of 3.89 calculated by Hess. Variational effects have a small impact in the calculated TST classical KIEs. The ZCT transmission coefficients practically keep the classical KIE unaltered, and therefore, the tunneling contribution to the reaction remains masked. This result may seem awkward because, in the ZCT case, the RTE is also close to the top of the barrier and we expect tunneling to be controlled by the curvature at the top of the barrier, which is given by the imaginary frequency. Its value is $\omega_H^{\ddagger} = 1315i$ cm^{-1} for hydrogen transfer and $\omega_D^{\ddagger} = 1080i$ cm^{-1} for deuterium transfer. The ratio between both frequencies is only 1.21, which is far from the expected value of $\sqrt{2}$, if we assume a pure hydrogen (deuterium) motion for this normal mode. This result indicates that the imaginary frequency normal mode also involves the motion of heavy atoms, so the ratio $\omega_H^{\ddagger}/\omega_D^{\ddagger}$ is far from the ratio of the masses, $\sqrt{m_D/m_H}$. At the same time it should be noticed that the ZCT transmission coefficients are calculated along the MEP, and that this path includes the displacement of all the internal degrees of freedom and not only the hydrogen (deuterium) coordinate. The KIE due to tunneling increases when the curvature along the reaction coordinate is included. The calculated KIEs are somewhat smaller than the experimental values but clearly show the tendency that, in this case, the large primary KIE is due to quantum tunneling.

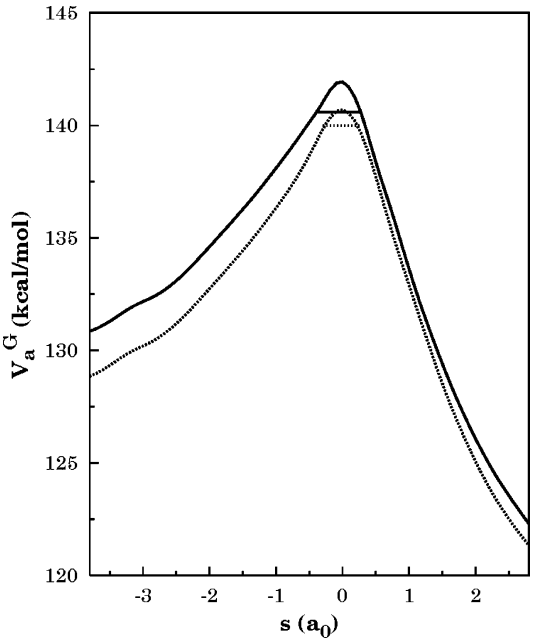

Figure 4. Ground-state vibrationally adiabatic potential for the hydrogen (solid line) and deuterium (dotted line) shift reactions of 7-methylocta-1,3(Z),5(Z)-triene. The straight lines indicate the representative tunneling energy at a temperature of $T = 333.2$ K.

TABLE 5: Factors in the KIEs[a]

T (K)	η_{var}	η_{int}	η_{cl}	η_{tun}^{ZCT}	$\eta_{tun}^{\mu OMT}$	η_{calc}	η_{exp}
298.2	0.99	4.34	4.30	1.09	1.55	6.8	
333.2	0.98	3.81	3.73	1.08	1.43	5.3	$7.0^{+1.3}_{-0.8}$
348.2	0.99	3.58	3.54	1.08	1.40	4.9	$6.5^{+0.7}_{-1.1}$
368.2	0.98	3.36	3.29	1.07	1.35	4.5	$5.2^{+0.9}_{-0.6}$
388.2	0.99	3.15	3.12	1.07	1.32	4.1	4.6 ± 0.6
400.0	0.99	3.03	3.00	1.06	1.29	3.9	

[a] The classical, η_{cl}, and total, η_{calc}, KIEs are given by eq 11 and eq 9, respectively. The experimental KIEs, η_{exp}, are taken from Baldwin and Reddy[8] considering a deviation of $E_a^D - E_a^H = 0.1$ kcal·mol^{-1}. The factors η_{tun}^{ZCT} and $\eta_{tun}^{\mu OMT}$ are also listed for comparison.

The above conclusions can be extrapolated to the [1,7] hydrogen shift in previtamin D_3, because this molecule has similar characteristics to the model system studied here. The KIEs measured by Okamura et al.[11] are similar to those obtained by Baldwin and Reddy for the hydrogen shift in 7-methylocta-1,3(Z),5(Z)-triene. The former author also measured an $E_a^D - E_a^H$ difference of 1.2 kcal·mol^{-1}, which is in very good agreement with our μOMT results for the model system.

4. Conclusions

The evaluation of thermal rate constants by high-level direct-dynamics CVT/μOMT calculations at the MPWB1K/DIDZ level has shown to be adequate to study the [1,7] sigmatropic hydrogen shift in 7-methylocta-1,3(Z),5(Z)-triene, which can be considered a model system for previtamin D_3. The calculated activation energies and primary KIEs are in reasonable agreement with the experimental data when quantum tunneling is taken into account. The CVT/μOMT calculations also indicate that it is important to consider the coupling between the reaction coordinate and the transverse modes to obtain KIEs comparable to the experimental values.

Acknowledgment. The authors thank Xunta de Galicia for Project No. 2003/PX199. A.F.-R., R.M.-P, E.M.-N., and S.A.V. thank the Ministerio de Educación y Ciencia (MEC) for project #BQU2003-01639. S.H.M. acknowledges financial support from Shiraz University during his Sabbatical leave. The authors also thank CESGA for computational facilities.

References and Notes

(1) Holick, M. F. *J. Cell. Biochem.* **2003**, *88*, 296.

(2) See for example: (a) Tian, X. Q.; Holick, M. F. J. *Biochem.* **1999**, *274*, 4174. (b) Dmitrenko, O.; Bach, R. D.; Sicinski, R. R.; Reischl, W. *Theor. Chem. Acc.* **2003**, *109*, 170. (c) Sheves, M.; Berman, E.; Mazur, Y.; Zaretskii, Z. V. I. *J. Am. Chem. Soc.* **1979**, *101*, 1882.

(3) *Isotope Effects in Chemistry and Biology*; Kohen, A, Limbach, H.-H., Eds.; Taylor & Francis (CRC): Boca Raton, FL, 2005.

(4) Smedarchina, Z; Siebrand, W.; Fernández-Ramos, A.; Cui, Q. *J. Am. Chem. Soc.* **2003**, *125*, 243.

(5) Alhambra, C.; Corchado, J. C.; Sánchez, M. L.; Gao, J.; Truhlar, D. G. *J. Am. Chem. Soc.* **2000**, *122*, 8197.

(6) González-Lafont, A.; Truong, T. N.; Truhlar, D. G. *J. Phys. Chem.* **1991**, *95*, 4618.

(7) Baldwin, J. E. ; Reddy, V. P. *J. Am. Chem. Soc.* **1987**, *109*, 8051.

(8) Baldwin, J. E. ; Reddy, V. P. *J. Am. Chem. Soc.* **1988**, *110*, 8223.

(9) Jensen, F. *J. Am. Chem. Soc.* **1995**, *117*, 7487.

(10) Hess, B. A., Jr. *J. Org. Chem.* **2001**, *66*, 5897.

(11) Okamura, W. H.; Elnagar, H. Y.; Ruther, M.; Dobreff, S. *J. Org. Chem.* **1993**, *58*, 600.

(12) Zhao, Y.; Truhlar, D. G. *J. Phys. Chem. A* **2004**, *108*, 6908.

(13) Hehre, W. J.; Ditchfield, R.; Pople, J. A. *J. Chem. Phys.* **1972**, *56*, 2257.

(14) Perdew, J. P. In *Electronic Structure of Solids '91*; Ziesche, P., Esching, H., Eds.; Akademie Verlag: Berlin, 1991; p 11.

(15) Becke, A. D. *J. Chem. Phys.* **1996**, *104*, 1040.

(16) Frisch, M. J.; Trucks, G. W.; Schlegel, H. B.; Scuseria, G. E.; Robb, M. A.; Cheeseman, J. R.; Montgomery, J. A., Jr.; Vreven, T.; Kudin, K. N.; Burant, J. C.; Millam, J. M.; Iyengar, S. S.; Tomasi, J.; Barone, V.; Mennucci, B.; Cossi, M.; Scalmani, G.; Rega, N.; Petersson, G. A.; Nakatsuji, H.; Hada, M.; Ehara, M.; Toyota, K.; Fukuda, R.; Hasegawa, J.; Ishida, M.; Nakajima, T.; Honda, Y.; Kitao, O.; Nakai, H.; Klene, M.; Li, X.; Knox, J. E.; Hratchian, H. P.; Cross, J. B.; Adamo, C.; Jaramillo, J.; Gomperts, R.; Stratmann, R. E.; Yazyev, O.; Austin, A. J.; Cammi, R.; Pomelli, C.; Ochterski, J. W.; Ayala, P. Y.; Morokuma, K.; Voth, G. A.; Salvador, P.; Dannenberg, J. J.; Zakrzewski, G.; Dapprich, S.; Daniels, A. D.; Strain, M. C.; Farkas, O.; Malick, D. K.; Rabuck, A. D.; Raghavachari, K.; Foresman, J. B.; Ortiz, J. V.; Cui, Q.; Baboul, A. G.; Clifford, S.; Cioslowski, J.; Stefanov, B. B.; Liu, G.; Liashenko, A.; Piskorz, P.; Komaromi, I.; Martin, R. L.; Fox, D. J.; Keith, T.; Al-Laham, M. A.; Peng, C. Y.; Nanayakkara, A.; Challacombe, M.; Gill, P. M. W.; Johnson, B.; Chen, W.; Wong, M. W.; Gonzalez, C.; Pople, J. A. *Gaussian 03*, revision B.01; Gaussian Inc.: Pittsburgh, PA, 2003.

(17) Truhlar, D. G.; Isaacson, A. D.; Garrett, B. C. In *Theory of Chemical Reaction Dynamics*; Baer, M., Ed.; CRC Press: Boca Raton, FL, 1985; Vol. 4, pp 65−137.

(18) Fernández-Ramos, A.; Ellingson, B. A.; Garrett, B. C.; Truhlar, D. G. *Rev. Comput. Chem.* **2007**, *23*, 124.

(19) Chuang, Y.-Y.; Truhlar, D. G. *J. Phys. Chem. A* **1998**, *102*, 242.

(20) Page, M.; McIver, J. W. *J. Chem. Phys.* **1988**, *88*, 922.

(21) Natanson, G. A.; Garrett, B. C.; Truong, T. N.; Joseph, T; Truhlar, D. G. *J. Chem. Phys.* **1991**, *94*, 7875.

(22) Jackels, C. F.; Gu, Z.; Truhlar, D. G. *J. Chem. Phys.* **1995**, *102*, 3188.

(23) Garrett, B. C.; Truhlar, D. G. *J. Chem. Phys.* **1979**, *70*, 1593.

(24) Garrett, B. C.; Truhlar, D. G. *J. Phys. Chem.* **1979**, *83*, 1079.

(25) Garrett, B. C.; Truhlar, D. G. *J. Phys. Chem.* **1979**, *83*, 3058.

(26) Lu, D.-h.; Truong, T. N.; Melissas, V. S.; Lynch, G. C.; Liu, Y.-P.; Garrett, B. C.; Steckler, R.; Isaacson, A. D.; Rai, N. S.; Hancock, G. C.; Lauderdale, J. G.; Joseph, T.; Truhlar, D. G. *Comput. Phys. Commun.* **1992**, *71*, 235.

(27) Bondi, D. K.; Connor, J. N. L.; Garrett, B. C.; Truhlar, D. G. *J. Chem. Phys.* **1983**, *78*, 5981.

(28) Garrett, B. C.; Joseph, T.; Truong, T. N.; Truhlar, D. G. *Chem. Phys.* **1989**, *136*, 271.

(29) Fernández-Ramos, A.; Truhlar, D. G. *J. Chem. Phys.* **2001**, *114*, 1491.

(30) Liu, Y.-P.; Lu, D. H.; González-Lafont, A.; Truhlar, D. G.; Garrett, B. C. *J. Am. Chem. Soc.* **1993**, *115*, 7806.

(31) Marcus, R. A.; Coltrin, M. E. *J. Chem. Phys.* **1977**, *67*, 2609.

(32) Fernández-Ramos, A.; Truhlar, D. G. *J. Chem. Theory Comput.* **2005**, *1*, 1063.

(33) Garrett, B. C.; Truhlar, D. G. *J. Chem. Phys.* **1983**, *79*, 4931.

(34) Allison, T. C.; Truhlar, D. G. In *Modern Methods for Multidimensional Dynamics Computations in Chemistry*; Thompson, D. L., Ed.; World Scientific: River Edge, NJ, 1998; pp 618−712.

(35) Corchado, J. C.; Chuang, Y-Y.; Coitino, E. L.; Truhlar, D. G. *GAUSSRATE*, version 9.1/P9.1-G03/G98/G94; Department of Chemistry and Supercomputer Institute, University of Minnesota: Minneapolis, MN, July 2003.

(36) Corchado, J. C.; Chuang, Y-Y.; Fast, P. L.; Villa, J.; Hu, W-P.; Liu, Y-P.; Lynch, G. C.; Nguyen, K. A.; Jackels, C. F.; Melissas, V. S.; Lynch, B. J.; Rossi, I.; Coitino, E. L.; Fernandez Ramos, A.; Pu, J.; Albu, T. V.; Steckler, R.; Garrett, B. C.; Isaacson, A. D.; Truhlar, D. G. *POLYRATE*, version 9.3; Department of Chemistry and Supercomputer Institute, University of Minnesota: Minneapolis, MN, Nov 2003.

(37) Peslherbe, G. H.; Hase, W. L. *J. Chem. Phys.* **1994**, *101*, 8535.

(38) Vereecken, L.; Peeters, J. *J. Chem. Phys.* **2003**, *119*, 5159.

(39) Kim, Y.; Truhlar, D. G.; Kreevoy, M. M. *J. Am. Chem. Soc.* **1991**, *113*, 7837.